RSC Advances

REVIEW

View Article Online
View Journal | View Issue

Cite this: *RSC Adv.*, 2023, **13**, 6518

Electrosorption performance on graphene-based materials: a review

Yan Liu, *[a] Yun Tian,[a] Jianda Xu,[a] Changfu Wang,[a] Yun Wang,[a] Dingzhong Yuan[a] and Jia Wei Chew *[bc]

Due to its unique advantages such as flexible planar structure, ultrahigh specific surface area, superior electrical conductivity and electrical double-layer capacitance in theory, graphene has unparalleled virtues compared with other carbon materials. This review summarizes the recent research progress of various graphene-based electrodes on ion electrosorption fields, especially for water desalination utilizing capacitive deionization (CDI) technology. We present the latest advances of graphene-based electrodes, such as 3D graphene, graphene/metal oxide (MO) composites, graphene/carbon composites, heteroatom-doped graphene and graphene/polymer composites. Furthermore, a brief outlook on the challenges and future possible developments in the electrosorption area are also addressed for researchers to design graphene-based electrodes towards practical application.

Received 27th December 2022
Accepted 19th February 2023

DOI: 10.1039/d2ra08252g

rsc.li/rsc-advances

1. Introduction

Traditional desalination technologies include membrane separation, electrodialysis, thermal separation and precipitation centrifugation.[1] These traditional technologies usually require expensive infrastructure, high energy consumption and easy to cause secondary pollution.[2] Therefore, new desalination technologies with low cost, low energy consumption, high efficiency and green production are urgently required.

Capacitive deionization (CDI) technology, also known as electro-sorption (EST) technology, is a novel water treatment technology that has attracted many researchers in recent years to achieve water purification/desalination.[3] Fig. 1 shows the advantages of capacitive deionization technology in wastewater treatment.[4] By applying a low potential (usually lower than 2 V), the charged ions are forced to the oppositely charged electrode and concentrated in the electric double layer (EDL) which is formed on the surface of the electrode.[5] A typical CDI cell is usually similar to the battery structure of a supercapacitor. It consists of a pair of electrodes separated by water and the aqueous solution is between/flow through the electrodes.[6] When an external potential is applied, the ions can migrate to the oppositely charged electrodes to form EDL. While the external potential is set to the opposite charge, the ions will withdraw from the electrodes to the feed solution.[7] Therefore, the ions can migrate directionally in the solution to be enriched and concentrated to achieve the purpose of ion separation and removal, as shown in Fig. 2.[8]

The concept of CDI was first proposed by Caudle and Johnson group in the 1960s.[9,10] They designed a CDI system using porous activated carbon electrodes, similar to supercapacitors, but due to the limitations of electrode materials, the technology has not been further developed. Until the 1970s, Johnson *et al.* conducted a reversible electrosorption model for activated carbon electrode regeneration,[10] and the concept of CDI has hardly improved. Later, the CDI process experienced a stage of rapid development on electrode materials, and the mechanism of which was attributed to the adsorption of ions in the EDL. In the past decade, the CDI process has been applied in many

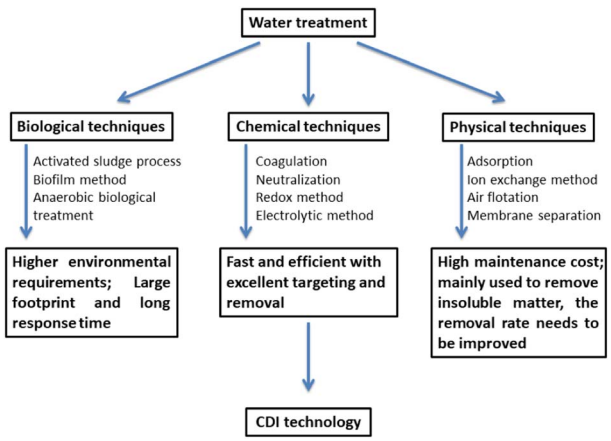

Fig. 1 Wastewater treatment and its solution through capacitive deionization technology.

[a]*Engineering Research Center of Nuclear Technology Application (East China Institute of Technology), Ministry of Education, Nanchang, 330013, China. E-mail: fzliuyan1986@163.com*

[b]*School of Chemical and Biomedical Engineering, Nanyang Technological University, Singapore 637459, Singapore. E-mail: JChew@ntu.edu.sg*

[c]*Singapore Membrane Technology Center, Nanyang Environment and Water Research Institute, Nanyang Technological University, Singapore 639798, Singapore*

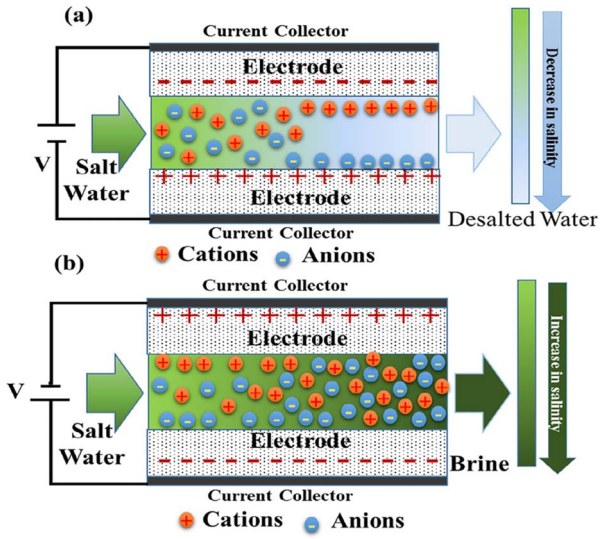

Fig. 2 Schematic diagram of a typical CDI system (a) deionization/desalination step (b) electrode regeneration steps. (Reproduced with permission from ref. 8 Copyright 2018 Elsevier.)

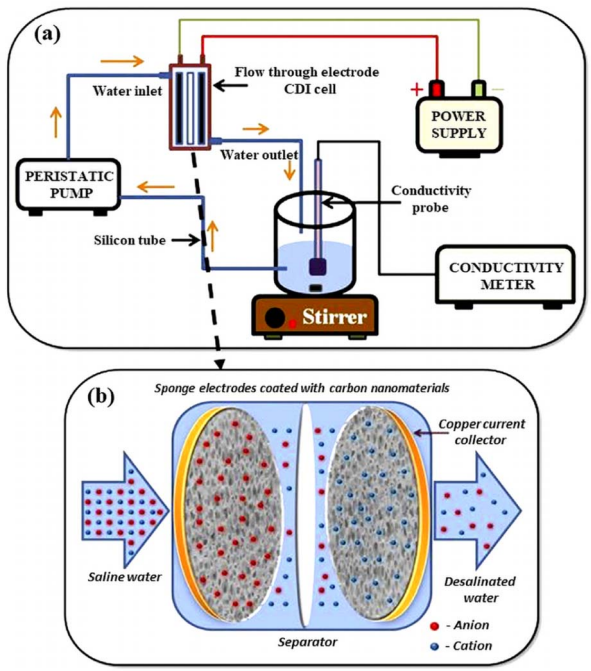

Fig. 3 (a) Schematic illustration for the CDI experimental set-up (b) working of CDI cell. (Reproduced with permission from ref. 47 Copyright 2018 Elsevier.)

fields, such as wastewater treatment and insulin purification due to its environmental friendliness, no secondary pollution and reduced energy consumption owning to the advantages of low capital cost, low driven energy, reliable regeneration and none secondary pollution.[11–14] Also, the technology has been advanced in many areas such as hybrid materials for electrode synthesis, flow electrodes,[15,16] flow-through electrodes,[17,18] and the relationship between surface properties and CDI efficiency, *etc.*

The electrode material is an important factor in CDI operation because the electrode material must have a large specific area, low resistance, suitable pore size distribution structure, good electrical conductivity and electrochemical stability, which are beneficial for the electrosorption capacity.[19] The process has to go through multiple steps of electrosorption and circulation. Therefore, the electrode should has not only good pore structure and reusability, but also wettability and hydrophilicity to ensure that all pores could participate in the adsorption process.[20–22] At the same time, a certain degree of scalability is essential so that the electrode material can be modified in some ways to optimize its performance in the future to enhance application potential.

In CDI system, different operation and structural parameters can affect the performance of CDI, such as applied voltage, flow rate of salt solution, initial concentration, salt adsorption capacity of electrode,[23] as well as ion selectivity and electrode thickness. The performance of ion selectivity depends on its affinity with functional groups.[24] Grafting the electrode surface with functional groups can improve the hydrophilicity of the electrode material, and also improve its electric adsorption capacity. Freire *et al.*[25] prepared Graphite Felt (GF) 3D composites and improved the performance of CDI by changing the electrode thickness on GF. The results of CDI experiments demonstrated that the values of salt adsorption capacity could be improved by more than 200% when reducing GF electrode thickness from 6.0 mm to 2.6 mm. Barcelos *et al.*[26] studied the effects of electrode thickness on the deionization performance. The results showed that the enhanced diffusion kinetics in a thin electrode with high intergranular porosity might play a decisive role in the selection of the optimal electrode for CDI applications.

Generally, the electrode, the heart of CDI, is generally fabricated with carbon materials, such as activated carbon,[27–29] porous carbon,[30–33] carbon aerogel,[34,35] carbon nanotubes,[36,37] graphene,[38] and the various carbon-based materials/composites.[39,40] In particular, graphene exhibits unique advantages such as flexible planar structure,[41] ultrahigh specific surface area (2600 $m^2 g^{-1}$), superior electrical conductivity (7200 m s^{-1} at room temperature) and electrical double-layer capacitance (21 μF cm^{-2}) in theory,[42] so it has unparalleled virtues compared with other carbon materials. In terms of supercapacitors, graphene meets the requirements of ideal capacitors, and its theoretical capacitance value reaches more than 200 F g^{-1}.[43] Therefore, graphene is highly expected in electrode application.

One of the preliminary reports of graphene for CDI application is the use of reduced graphene oxide (rGO) to produce graphene nanoflakes.[44,45] The specific surface area of the exfoliated graphene nanoflake was 222.01 $m^2 g^{-1}$, and the salt adsorption capacity was 4.30 mg g^{-1}.[46] For decades, researchers have developed different ways to use graphene as CDI electrodes. For instance, J. Ahirrao *et al.*[47] investigated the electrosorption performance of various carbon-based materials including carbon fabric (CF), functionalized-multiwall carbon nanotubes (F-MWCNT) and solar reduced graphene oxide

(SRGO) (Fig. 3). The outcome demonstrated that high electrosorption capacity of 10.70, 31.22 and 37.54 mg g^{-1} have been achieved with CF, F-MWCNT, and SRGO electrodes, respectively, under 1.4 V and 900 mg L^{-1} condition. Among all the electrodes studied, SRGO has the highest electrosorption capacity, followed by F-MWCNT and CF.

However, the electrosorption performance of graphene synthesized from the reduction method is not ideal in CDI process due to the re-stacking of graphene sheets because of van der Waals and π–π interactions.[48,49] Meanwhile, part of the reason why the electrosorption properties of ordinary graphene materials are so poor is due to their hydrophobicity. Hence, there are some approaches to enhance the electrosorption capacity of pristine graphene materials by adjusting intrinsic pore structure or improving the surface chemistry, such as fabricating 3D structure or introducing additional components, typically metal oxide or polymer.[50]

There is still a review gap in the field of modified graphene electrode materials. To fill this vacancy, we summarized the graphene-based electrodes for electrosorption reported in the literature for recent five years and categorized them into five parts: 3D graphene, graphene/metal oxide (MO) composites, graphene/carbon composites, heteratoms-doped graphene and graphene/polymer composites, which are more detailed than the previous reviews, and also laid a foundation for the future development and application of graphene-based electrodes.

2. Modification methods

2.1 3D graphene

In order to solve the stacking problem of graphene sheets, fabricating 3D structures for graphene is applicable. The porous structure of interconnection can change the volume of pores and provide paths for ion transfer.[51,52] In addition, a continuous skeleton of interconnected graphene sheets enables rapid electron transfer.[41,53] The 3D graphene can be used directly as an electrode without rebuilding the electrode passes through the adhesive, thus retaining the 3D structure can maximize its advantages. Different 3D forms of graphene, such as 3D composites, graphene hydrogel or graphene agrogel[54–59] have been reported to overcome the shortcomings of graphene and enhanced the electrosorption capacity.

Chang *et al.*[60] designed a honeycomb type of graphene clusters (HGC) and the electrosorption capacity was 14.08 mg g^{-1} with continuous circulation of 28 mL 5 mM NaCl solution (Fig. 4). Zhang's group[61] developed a 3D intercalated graphene sheet ball nanocomposite (GSSNA) by using graphene oxide and [Ni_2(EDTA)] as precursors. The electrosorption capacity of 22.09 mg g^{-1} was achieved in 500 mg per L NaCl solution at 1.2 V, and the salt removal efficiency was 90% (Fig. 5). Much work have been focused on salty water electrosorption, but the separation and recovery of heavy metal from wastewater by 3D

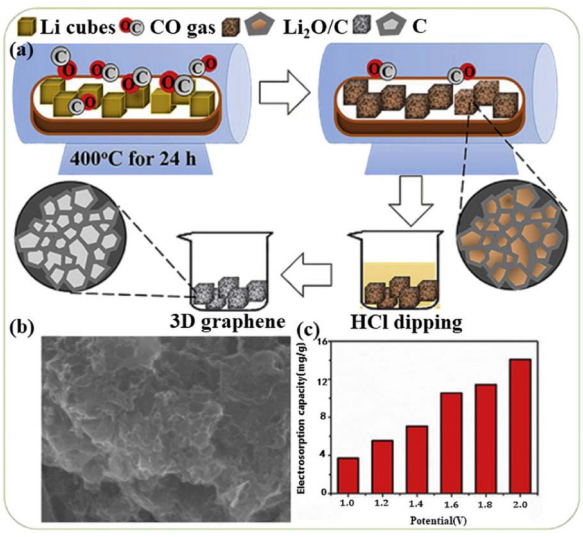

Fig. 4 (a) Schematic synthesis process of HGC; (b) SEM image of HGC; (c) electrosorption capacities at different potentials of HGC in a batch-mode circulation system at a flow rate of 10 mL min^{-1} (NaCl concentration of 5 mM). (Reproduced with permission from ref. 60 Copyright 2019 Elsevier.)

Fig. 5 Schematic representation of the fabrication of GSSNA. (Reproduced with permission from ref. 61 Copyright 2018 Royal Society of Chemistry.)

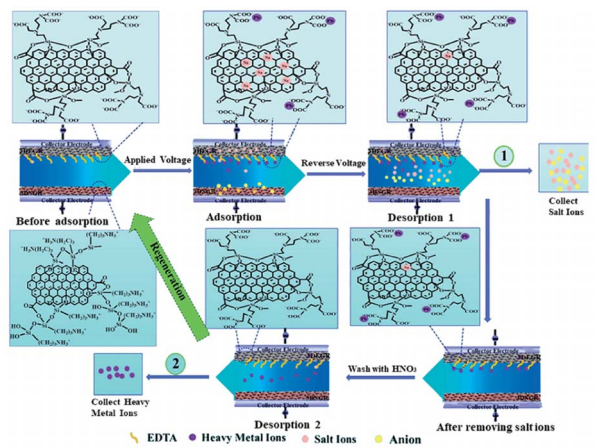

Fig. 6 Schematic illustration of separation and recovery of heavy metal ions and salty ions from wastewater by 3DEGR and 3DNGR. (Reproduced with permission from ref. 62 Copyright 2017 Royal Society of Chemistry.)

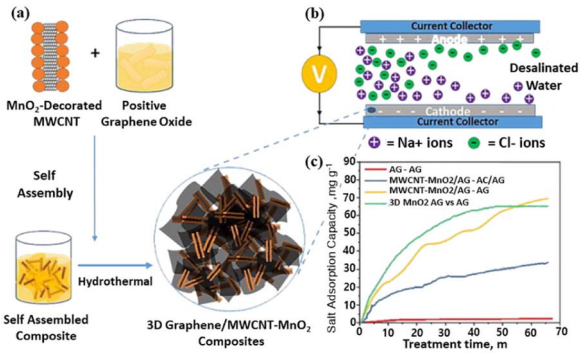

Fig. 7 (a) Schematic illustration of synthesizing the 3D nanocomposites; (b) schematic figure showing CDI working electrode; (c) salt adsorption capacity of MWCNT–MnO_2 and 3D composite. (Reproduced with permission from ref. 68 Copyright 2022 Elsevier.)

graphene can also be effective. Liu *et al.*[62] explored two 3D graphene-based electrodes (3DEGR and 3DNGR) and used as cathode and anode, respectively. The removal efficiency for Pb^{2+} and Na^{+} reached 99.9% and 98.7%, respectively (Fig. 6).

In addition, some layered pore structures including micropores, mesopores and macropores have been introduced into these 3D graphene-based material, which are conducive to ion diffusion and transmission, and enhance the electrosorption capacity.[63–66] However, because of the inherent barrier properties of graphene, the diffusion of ions in the micro/mesopores materials and the storage of brine in the macropores are hindered, thereby reducing the desalination performance of 3D-based graphene materials. Note that, Wang's group[67] designed a sample named 3DGA-OP with overall openness and

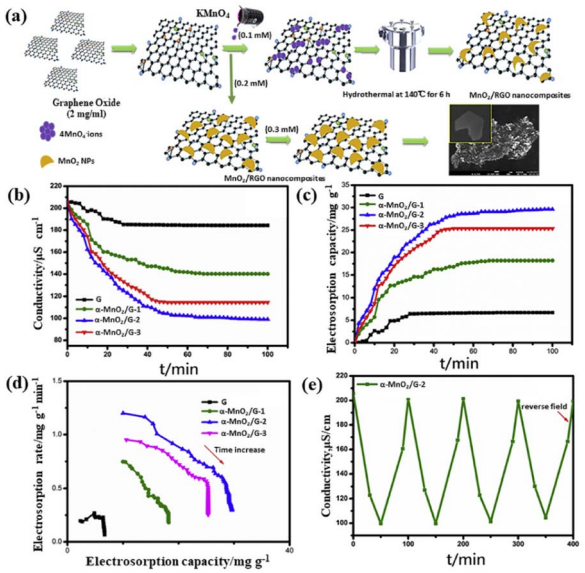

Fig. 8 (a) Illustration of the nucleation growth mechanism of MnO_2/G nanocomposites; (b) plots of conductivity *vs.* time; (c) electrosorption capacity *vs.* time; (d) CDI Kim–Yoon plots for G, α-MnO_2/G-1, α-MnO_2/G-2, and α-MnO_2/G-3 electrodes; (e) desalination–regeneration profile of the α-MnO_2/G-2 in a 100 mg per L NaCl at 1.2 V with a flow rate of 10 mL min^{-1}. (Reproduced with permission from ref. 76 Copyright 2020 Elsevier.)

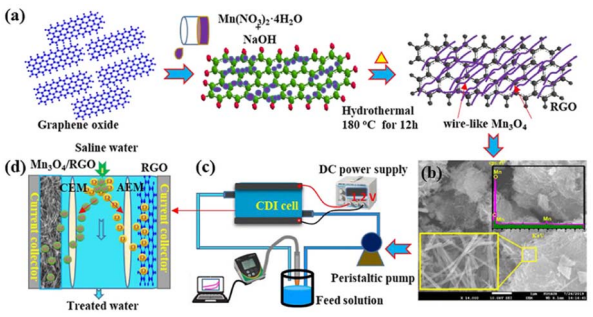

Fig. 9 (a) Schematic diagram of the formation of Mn_3O_4/RGO; (b) FE-SEM image and EDS of Mn_3O_4/RGO; schematic diagram of CDI (c) set-up and (d) mechanism using Mn_3O_4/RGO. (Reproduced with permission from ref. 77 Copyright 2020 Elsevier.)

interconnection structure. The CDI capacity reached 14.4 mg g^{-1} in NaCl aqueous solution of 500 mg L^{-1} at 1.2 V. Wadi *et al.*[68] prepared a 3D nanocomposite by embedding MWCNT–MnO_2 between interconnected graphene layers with salt adsorption capacity of 65.1 mg g^{-1} observed under 1.2 V and 600 ppm NaCl solution. The excellent electrosorption performance was attributed to the architecture and pseudo-capacitive behavior (Fig. 7).

2.2 Graphene/metal oxide (MO) composites

Most of the synthetic routes for 3D graphene-based electrodes involves templated synthesis, which is complicated, time consuming and cost-effective. In addition, the desalination performance should be further improved to meet the requirements of practical applications. To solve the shortcomings caused by 3D graphene, one of the methods is to develop graphene/MO composites.[69–72] It is reported that the combination of graphene and MO possess high specific capacitance, high density of active surface sites, exceptional chemical stability, wettability and charge efficiency, and reduce the aggregation of graphene sheets and increase the interplanar spacing.[7,73–75] Jaoude *et al.*[76] fabricated shrimp-like α-MnO_2/graphene (α-MnO_2/G) nanocomposite due to the auxiliary pseudo-capacitance behavior of MnO_2. The authors studied the influence of MnO_2 morphology on the electrochemical

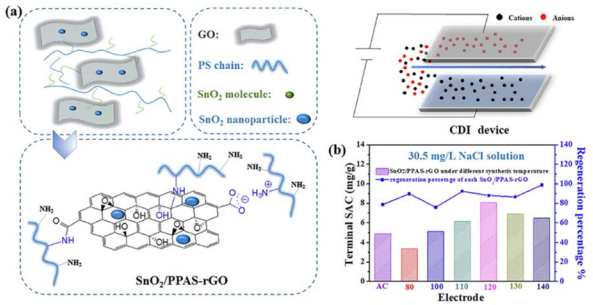

Fig. 10 (a) The schematic diagram of the synthetic route of SnO_2/PPAS-rGO; (b) the terminal SAC and regeneration percentage of SnO_2/PPAS-rGO electrode. (Reproduced with permission from ref. 78 Copyright 2021 Elsevier.)

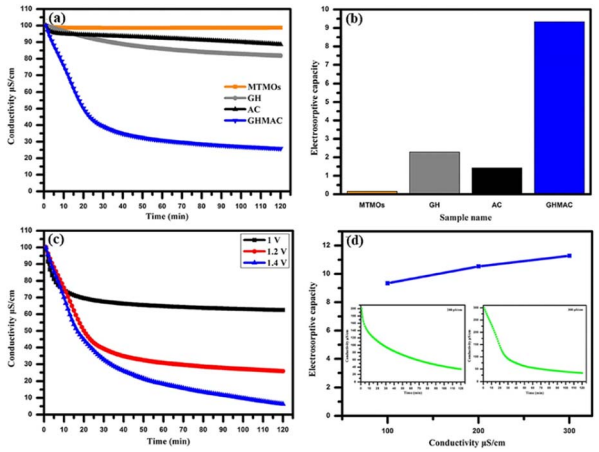

Fig. 11 (a) CDI performance at different time; (b) electrosorption capacity of GHMAC electrode; (c) CDI performance at different applied voltages; (d) electrosorption capacity at different concentrations (the inset figure for CDI performance at 200 and 300 μS per cm NaCl) of GHMAC electrode. (Reproduced with permission from ref. 7 Copyright 2019 Elsevier.)

performance of the electrode and the capacitive deionization performance. The established hybrid battery could provide up to 375 F g^{-1} capacitance at 10 mV s^{-1} and showed reversible salt insertion/reverse insertion capacity up to 29.5 mg g^{-1} at 1.2 V (Fig. 8). Various oxidation states of manganese such as Mn_3O_4 is also a potential candidate for CDI electrode. Later, this group[77] introduced a layered network architecture of pseudo-capacitive Mn_3O_4 nanowires fixed on reduced graphene oxide (Mn_3O_4/RGO) hybrid. The electrosorption capacity (SAC) of the electrode was 34.5 mg g^{-1} at 1.2 V with a salt adsorption rate (ASAR) of 1.15 mg (g min)$^{-1}$ in 1000 mg per L NaCl solution (Fig. 9).

SnO_2 can accelerate the charge transport and provide sites for activated adsorption, moreover, the stability and electrosorption efficiency might decrease during practical water current, Xie *et al.*[78] developed SnO_2 and aminated polystyrene co-functionalized GO composites (SnO_2/PPAS-rGO). The composites presented electrosorption capacity of 8.07 mg g^{-1} at 1.8 V with a flow rate of 20 mL min^{-1} in 30.5 mg per L NaCl solution (Fig. 10).

The oxidation state of Ce can provide direct, rapid and convenient mutational transformation between Ce(III) and Ce(IV), thereby promote fast electron transport and cerium ion diffusion.[79,80] Therefore, Yousef *et al.*[81] used CeO_2 intercalated between graphene to improve the electrosorption capacity and the electrode showed 7.2 mg g^{-1} electrosorption capacity with 65% removal efficiency. Yasin *et al.*[7] took the advantage of 3D graphene, activated carbon and mixed MO (including TiO_2 and ZrO_2) (GHMAC) *via* an electrospinning technique. The composite showed 9.34 mg g^{-1} electrosorption capacity at the initial solution conductivity of 100 μS cm^{-1} (Fig. 11).

2.3 Graphene/carbon-based composites

In the other hand, incorporating metal oxides, metal hydroxides or conducting polymers may not be suitable for practical applications because of the high cost, complex synthetic

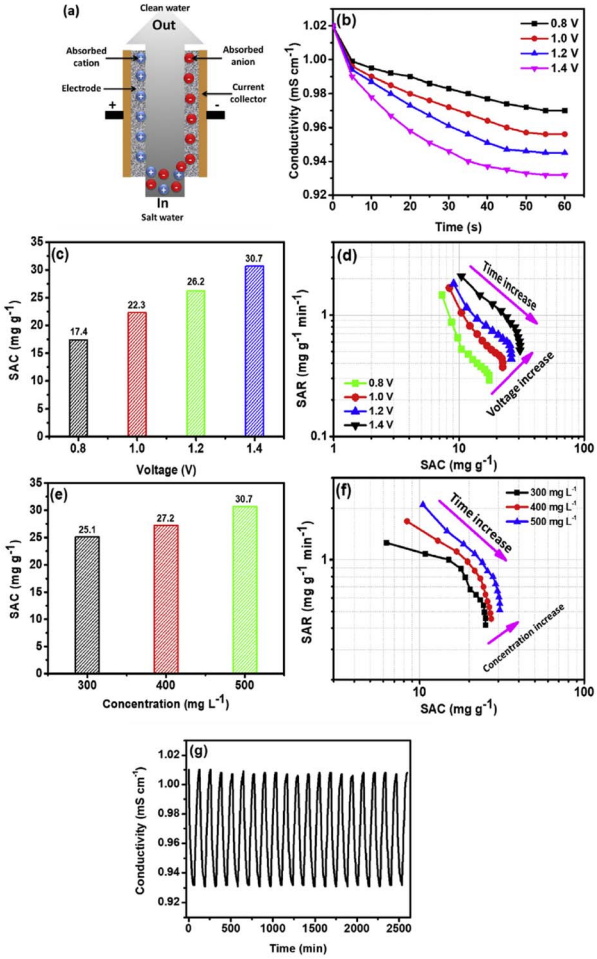

Fig. 12 (a) Schematic illustration of CDI; (b) conductivity of NaCl Vs time plot; (c) electrosorption capacity for different voltages at 500 mg per L NaCl concentration and flow rate of 25 mL min^{-1}; (d) CDI Ragone plot; (e) salt adsorption capacity for different concentrations at 1.4 V under flow rate of 25 mL min^{-1}; (f) CDI Ragone plot and (g) regeneration performance of CN–GS electrode. (Reproduced with permission from ref. 86 Copyright 2019 Elsevier.)

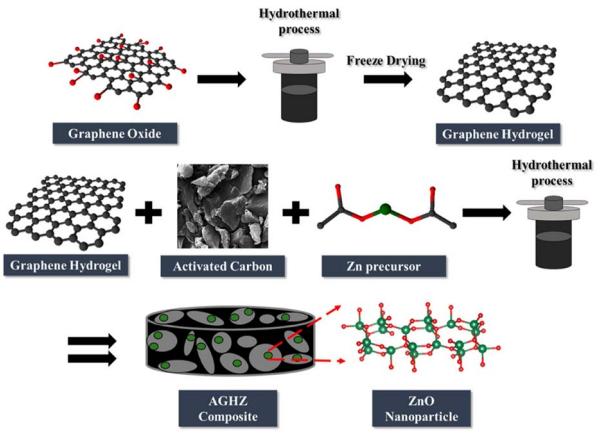

Fig. 13 Schematic illustration of the AGHZ nanocomposite. (Reproduced with permission from ref. 88 Copyright 2021 Elsevier.)

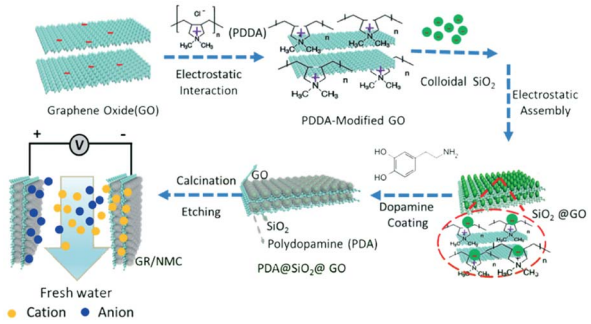

Fig. 14 Schematic illustration of the sandwich-like nitrogen-doped graphene composites. (Reproduced with permission from ref. 92 Copyright 2018 Royal Society of Chemistry.)

technology and poor electrochemical stability. Another applicable way to improve the electrosorption capacity of electrodes is to combine different carbon-based materials with various structural characteristics and physicochemical properties which may obtain joint effect on the performance.[82] The composites of carbon-based materials and graphene have been shown to be a new method to improve the electrosorption capacity of graphene because the inserted carbon-based materials act as a conductive network and inhibit graphene sheet aggregation.[15,83]

Chong *et al.*[84] fabricated GAC composite by dispersion of activated carbon in graphene and the electrosorption efficiency of the electrode increased from 1.6% to 3.0% in the regeneration cycles under +1.2 → 0 → +1.2 V while the efficiency of the activated carbon electrode decreased from 2.7% to 1.6%. Zhang *et al.*[85] prepared graphene/carbon aerogels composite (GCCAS) and the best electrosorption capacity was 26.9 mg g^{-1} and 18.9 mg g^{-1} in NaCl solutions with concentrations of 500 mg L^{-1} and 250 mg L^{-1}, respectively.

Mohanapriya *et al.*[86] reported the synthesis of graphene/carbon nanoparticles composite (CN–GS). The electrosorption capacity of CN–GS was 30.7 mg g^{-1} in 500 mg per L NaCl solution with excellent cycle stability above 500 cycles (Fig. 12). Cao *et al.*[87] modified 3D graphene hydrogel with single-walled

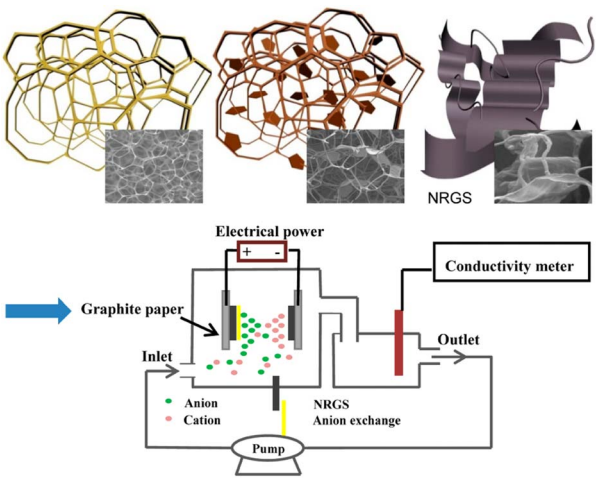

Fig. 15 Schematic diagram of the fabrication of NRGS electrodes. (Reproduced with permission from ref. 97 Copyright 2017 American Chemical Society.)

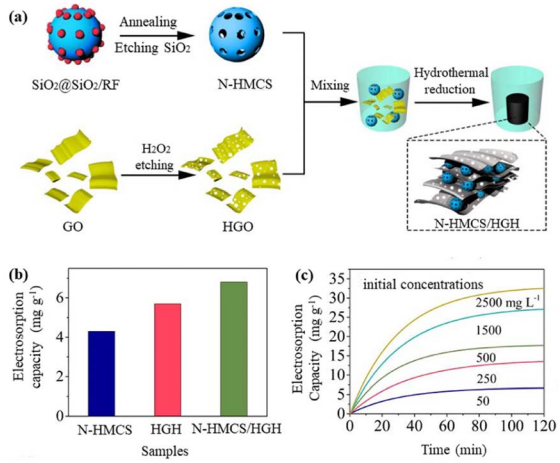

Fig. 16 (a) Schematic diagram of the synthesis of N-HMCS/HGH composite; (b) electrosorption capacity at an initial concentration of 50 mg L^{-1}; (c) time-dependent electrosorption capacity for the N-HMCS/HGH electrode of NaCl solutions with different initial concentrations. (Reproduced with permission from ref. 98 Copyright 2019 Elsevier.)

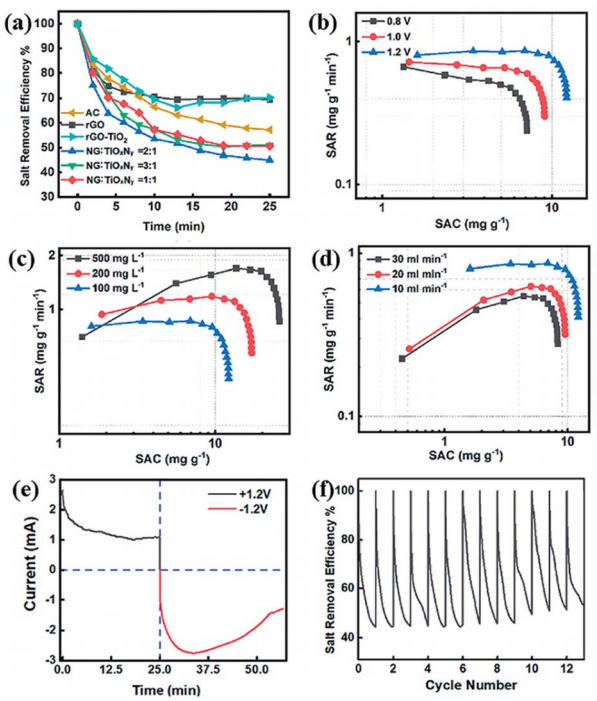

Fig. 17 (a) Comparison of salt retention curves of electrodes NG : TiO_xN_y = 1 : 1 to 3 : 1, rGO, and AC; Ragone plots of NG–TiO_xN_y at: (b) potential of 0.8 V, 1.0 V and 1.2 V; (c) water salinity of 500 mg L^{-1}, 200 mg L^{-1}, and 100 mg L^{-1}; (d) flow rates of 30 mL min^{-1}, 20 mL min^{-1} and 10 mL min^{-1}; (e) current *vs.* time plot; (f) cycling stability for over 12 cycles. (Reproduced with permission from ref. 107 Open access from 2019 Royal Society of Chemistry.)

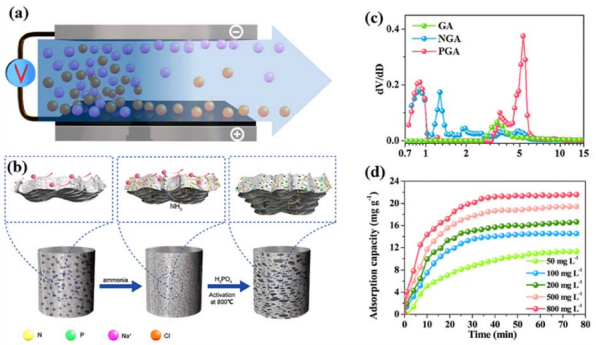

Fig. 18 Schematic illustration of (a) the process of CDI; (b) preparing samples; (c) pore size distribution of PGA; (d) adsorption capacity variation of PGA electrodes in NaCl solution at different initial concentration. (Reproduced with permission from ref. 111 Copyright 2020 Elsevier.)

CNT and multi-walled CNT. The results showed that SWCNTs/rGO has a higher electrosorption capacity (48.73 mg g^{-1}) higher than MWCNTs/rGO due to its higher specific surface area (308.37 m^2 g^{-1}). Yasin *et al.*[88] fabricated a graphene hydrogel and zinc oxide nanoparticles incorporating activated carbon composite (AGHZ) with a specific capacitance of 746.5 F g^{-1} at 10 mV s^{-1}, salt removal efficiency of 83.65% and electrosorption capacity of 9.95 mg g^{-1} (Fig. 13).

2.4 Heteratoms-doped graphene

So far, different methods have been developed to prevent re stacking of graphene nanosheets during electrode fabrication to improve the electrosorption abilities in CDI applications.[89] Consequently, one way is to synthesize graphene using various guest materials such as mesoporous carbon, carbon nanotubes or activated carbon to insert into the interlayer of graphene to prevent agglomeration.[90,91] In this way, the CDI capacity of the modified graphene electrode can be increased to 0.83–3.23 mg g^{-1}. These materials show higher specific surface

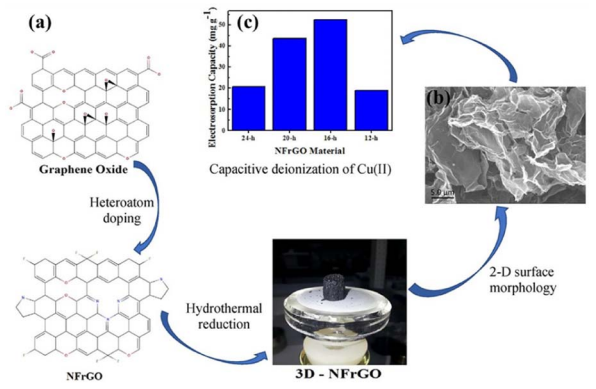

Fig. 19 (a) Illustration of fabrication of 3-dimensional N, F-codoped reduced graphene oxide (NFrGO); (b) SEM image of NFrGO fabricated at 16 h; (c) copper electrosorption capacity of NFrGO electrode materials after 120 min of incubation in CDI system. (Reproduced with permission from ref. 112 Copyright 2021 Elsevier.)

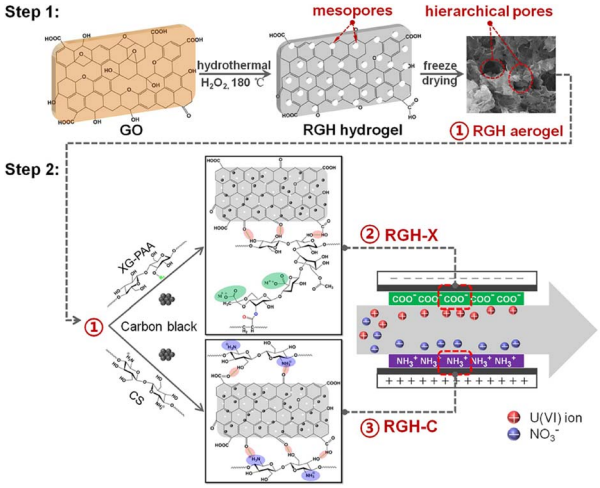

Fig. 20 Schematic of preparation route of polysaccharide-bound RGH electrodes for uranium electrosorption. (Reproduced with permission from ref. 114 Copyright 2021 Elsevier.)

area and unique "plane-to-line" or "plane-to-plane" networks, which are beneficial for improving the overall conductivity and ion transmission.[92]

However, the pure carbon materials have poor wettability due to the hydrophobicity of the guest carbon material, and result into the hindrance of internal ion diffusion. Therefore, it is essential to improve the wettability and hydrophilicity of the carbon electrodes. It is reported that doping methods have been widely used to improve the conductivity and permeability of carbon materials. In particular, the most attractive dopant is nitrogen due to its smaller atomic radius and higher electronegativity (3.5) compared to carbon (3.0).[93] Nitrogen-doping can

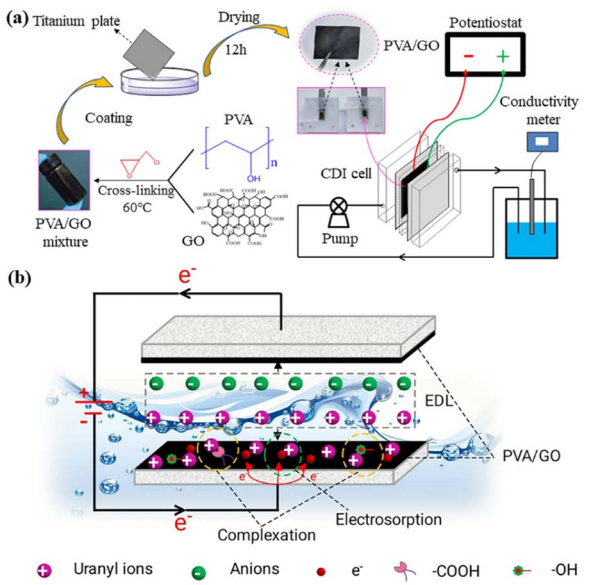

Fig. 21 (a) The preparation route for PVA/GO and the system for CDI; (b) possible U(VI) electrosorption mechanism for PVA/GO-4. (Reproduced with permission from ref. 116 Copyright 2021 Elsevier.)

produce n-type conductivity which can induce a lot of defects, so it can improve conductivity and wettability without changing their morphology merits.[94–96]

For example, Zhang's group[92] designed a sandwich-like nitrogen-doped graphene composite as a CDI electrode through a self-assembly strategy. This structure provided high specific surface area and excellent conductivity with wettability. The electrode showed a salt adsorption capacity of up to 18.4 mg g^{-1} in a 500 mg per L NaCl aqueous solution with a high charging efficiency of 0.67 at 1.2 V and ideal recycling performance (Fig. 15). Wang's group[97] used melamine sponge to prepare a new type of nitrogen-doped reduced graphene sponge composite (NRGS). The composite (A-NRGS) was prepared by coating the surface of the NRGS electrode with quaternized modified (C-qPVA) cross-linked polyvinyl alcohol. The electrochemical capacity of A-NRGS composite was 184 F g^{-1} and the membrane capacitance deionization (MCDI) performance was 11.3 mg g^{-1} (Fig. 14).

Hu *et al.*[98] reported the construction of a layered porous composite of N-doped composite namely N-HMCS/HGH. The electrode has a specific capacitance of about 226.5 F g^{-1} in 0.5 M NaCl solution and the electrosorption capacities were 17.8 and 32 mg g^{-1}, respectively with initial concentrations of 500 and 2500 mg L^{-1}. After 35 regeneration cycles, the electrode showed cycling stability (Fig. 16). Li *et al.* found that after N doping, the electrosorption capacity of HMCS in 500 mg per L NaCl solution increased from 13.5 to 16.66 mg g^{-1}.[99] Liu *et al.* synthesized N-doped carbon nanorods from nanocrystalline cellulose, with an electrosorption capacity of 17.62 mg g^{-1}.[100–103]

Recently, researchers found that titanium oxynitride (TiO_xN_y, where x and y stand for the unspecific atom ratios of O and N to Ti) can be used as electrodes in batteries and supercapacitors due to the increased electrochemical ability.[104,105] In result, TiO_xN_y can be used as additives to enhance the electrical performance of graphene.[106] Chen's group[107] first reported the fabrication of nitrogen-doped graphene and TiO_xN_y nanocomposite (NG–TiO_xN_y). The salt adsorption capacity was 26.1 mg g^{-1} in 500 mg L^{-1} salt water, and retained its initial desalination efficiency over 90% after 12 regeneration cycles. The authors claimed that the layered graphene promoted the ions diffusion and formed electric double layer, while the presence of TiO_xN_y enhanced the electrochemical performance of electrodes by increasing surface area and vacancies created by nitriding (Fig. 17). Khalil *et al.*[108] developed N-doped and TiO_2 modified graphene oxides. The results showed that the specific capacitance was 157 F g^{-1} at 5 mV s^{-1} and 1.0 M NaCl, while pure graphene oxide was 19.5 F g^{-1}. The electrosorption capacity and the salt removal efficiency were 9.2 mg g^{-1} and 98%, respectively.

Other doping atoms such as sulfur, phosphorous can also produce external defects to enhance the electrochemical performance of graphene electrodes.[109,110] Han *et al.*[111] designed N and P-doped 3D graphene (NGA and PGA) with high conductivity and capacitance for CDI, which had specific surface area of 567.14 m^2 g^{-1} and capacitance of 177.19 F g^{-1} due to the 3D hierarchical porous structure and highly cross-linked networks of graphene sheets. The structure enhanced its desalination capacity up to 20.93 mg g^{-1} and maximum capacity of 30.92 mg g^{-1} (Fig. 18). Mamaril *et al.*[112] fabricated a N and F doped 3D rGO (3D-NFrGO) through hydrothermal rout with a 95% percent removal and specific electrosorption capacity of 52.3 mg g^{-1} for Cu^{2+} due to doping heteratoms, high surface area and pore structure. The results demonstrated that chemisorption and ion diffusion govern the Cu^{2+} removal (Fig. 19).

2.5 Graphene/polymer-based composites

In addition to water desalination, CDI technology can be used to recover radionuclide ions from aqueous solutions, such as U(VI).[113] However, a problem limiting the electrosorption performance of U(VI) is the poor hydrophilicity of the electrodes due to the use of hydrophobic polymer binders. In order to fabricate the integrated conductive networks, polymer binders, *i.e.* polyvinylidene difluoride (PVDF), are widely utilized during the preparation of electrodes which may hinder the ions penetrate diffuse into the internal structure, thus leading to the decreasing of U(VI) removal. To solve this issue, Liao *et al.*[114]

Table 1 Electrosorption properties of graphene-based electrodes

S. no.	Electrode material	Voltage [V]	NaCl concentration (mg L^{-1})	Flow rate (mL min^{-1})	Specific surface area (m^2 g^{-1})	Specific capacitance (F g^{-1})	Conductivity (μS cm^{-1})	Electrosorption capacity (mg g^{-1})	Ref.
1	3D-NFrGO	1.2	500	—	182.7	245.6	—	52.4	112
2	3D graphene/MWCNT–MnO_2 composites	1.2	600	10	312.2	19.02	—	65.1	68
3	α-MnO_2/G	1.2	500	10	—	375	145.3	29.5	76
4	Mn_3O_4/RGO	1.2	1000	5	160	437	150	34.5	77
5	SnO2/PPAS-rGO	1.8	500	20	141	58.0	57.24	8.07	78
6	GHMAC	1.2	1000	—	—	453	100	9.34	7
7	GCCAS	1.5	500	25	546.2	—	—	26.9	85
8	NRGS	1.6	1000	10	241	184	300	11.3	97
9	N-HMCS/HGH	1.4	500	—	337.7	226.5	—	32	98
10	NG–TiO_xN_y	1.2	500	10	64.22	84.8	—	26.1	107
11	GR/NMC	1.4	500	—	918	57.2	—	18.4	92

designed polysaccharides xanthan gum (XG)- and chitosan (CS) -bound porous graphene electrodes (RGH) which gave rise to 97.9% removal ratio within 4 h at 1.2 V for U(VI). Due to the introducing of polysaccharide adhesive, the groups with opposite charges on the surface of the positive and negative electrodes weakened the co-ionic repulsion effect, and gave them with excellent surface hydrophilicity and conductivity, which was conducive to the electrosorption of U(VI). At the same time, the negatively charged carboxylate group can attract U(VI) cations and form a stronger complex. The accumulated electrosorption capacity of RGH-X/RGH-C reached 1413.0 mg g^{-1} in six cycles, which was 75% higher than the PVDF-bound RGH electrodes (Fig. 20).

Similarly, poly(vinyl alcohol) (PVA), a hydrophilic material with superior biocompatible and non-toxic properties, contains abundant –OH groups and therefore can be used to enhance the hydrophilicity of the electrodes.[115] Thus, Tang *et al.*[116] fabricated PVA/GO composites for U(VI) electrosorption, which could utilize the hydrophilicity of PVA, enhance the dispersion ability of GO and maintain the excellent conductivity of GO (Fig. 21). The results showed that the removal efficiency of PVA/GO-4 (PVA : GO = 1 : 2) was 95.27% and the electrosorption capacity reached 29.2 mg g^{-1} at 0.9 V for U(VI).

The electrosorption properties of recent progress done on graphene-based materials mentioned above are summarized detailed in Table 1.

3. Conclusions and prospects

CDI is an ion removal technology that drives various ions by applying electricity. The ions are taken into the charged porous electrode and are stored in the porous structure of the electrode. Compared to traditional ion removing methods, developing electrodes with mechanical flexibility, energy efficiency and cost-effectiveness are key factors in recent advances in CDI technology.[6] There are still several limitations of developing graphene-based CDI electrode in practical applications.

For example, as to graphene/transition metal oxide composite, future works have been focused on complex oxides with large number of electrons in outer d orbitals such as $FePO_4$ (ref. 117) or $Na_4Ti_9O_{20}$ (ref. 118) to utilize external electronics to enhance the characteristics of composites such as conductivity. However, we should take the contamination caused by the metal oxides into consideration. In addition, water electrolysis and other parasitic redox reaction (such as reducing the dissolved oxygen in water, oxidation of carbon surface) may occur when graphene/metal oxide composites are used because the metal oxides may change the electrodes' zero charge potential to be close to the potential for parasitic redox reactions.[8]

Besides, the practical environment using the CDI devices should be taken into consideration.[119] The electrodes also show great adsorption capacity for natural organic substances. In the presence of natural organics, the electrode scales, the surface area of the electrode decreases, and the desalting performance of CDI is significantly reduced, and decreases with the increase of the concentration of natural organics.[120] This is mainly because the deposition of natural organic matter changes the adsorption position, resistance and capacitance characteristics of the electrodes.[121] After applying voltage/current, natural organics are adsorbed by electrode along with target ions simultaneously, resulting in the loss of adsorption capacity.

Another key problem is the electrosorption capacity of graphene-based electrodes is still low. Therefore, future research should focus on how to optimize certain parameters to improve the electrosorption performance, but for decades, the space for increasing the electrosorption capacity is still very limited. As a general technology, CDI can also be used for electrosorption of heavy metal ions or nuclide ions.[122–127] How to selectively remove specific ion using CDI technology is also an challenge in the future. Specific adsorption is important for recycling and enrichment of different ions. Literature have shown that electrosorption capacity of traditional graphene-based electrodes can be effectively improved through modifications which can achieve the selectivity to some extent.

Cycling stability also is an important parameter for practical CDI applications.[128] With the increase of the number of cycles, the stability and thermodynamic efficiency of graphene-based electrodes will also decrease. In the process of electrode preparation, due to the strong π–π bond and van der Waals force make graphene easy to easy to stack, resulting in the reduction of the spacing between nano-sheets, impeding the penetration of electrolyte, and thus reducing the desalination rate.[129] In another hand, chemical modification of graphene-based electrodes can induce physical and chemical adsorption, so the development potential of electrosorption capacity is enormous. However, oxygen-containing functional groups are acknowledged for enhancing capacitance.[130] The surface area of some electrodes may reduce after modification. Thus, the inconsistency should be balanced in the future research.

In short, CDI is a promising technology though many challenges still exist and the search for improved flexible graphene-based electrodes is continuing. How to solve these problems through the research about graphene-based electrode materials and accelerate the development process of CDI technology in different fields is a key issue that need to be studied in the future.

Author contributions

Yan Liu (drafting and paper writing); Yun Tian (drafting); Changfu Wang (data analysis); Yun Wang (resources and supervision); Dingzhong Yuan (resources and data analysis); Jia Wei Chew (reviewing the paper).

Conflicts of interest

The authors declare no competing financial interest.

Acknowledgements

We appreciate the financial support from the National Natural Science Foundation of China (22166001, 2216060121, 21966005), the Natural Science Foundation of Jiangxi Province (20224BAB203005), College Students' Innovation and

Entrepreneurship Training Program of Jiangxi Province (S202210405025), Engineering Research Center of Nuclear Technology Application of East China Institute of Technology (HJSJYB2022-8).

References

1 J. Ma, G. Qin, W. Wei, T. Xiao, L. Jiang and S. Liu, *Desalination*, 2020, **476**, 114232.
2 K. Elsaid, M. Kamil, E. T. Sayed, M. A. Abdelkareem, T. Wilberforce and A. Olabi, *Sci. Total Environ.*, 2020, **748**, 141528.
3 P. Liu, T. Yan, L. Shi, H. S. Park, X. Chen, Z. Zhao and D. Zhang, *J. Mater. Chem. A*, 2017, **5**, 13907–13943.
4 H. Chen, M. Huang, Y. Liu, L. Meng and M. Ma, *Sci. Total Environ.*, 2020, **739**, 139944.
5 Z. Huang, L. Lu, Z. Cai and Z. J. Ren, *J. Hazard. Mater.*, 2016, **302**, 323–331.
6 Q. Dong, X. Guo, X. Huang, L. Liu, R. Tallon, B. Taylor and J. Chen, *Chem. Eng. J.*, 2019, **361**, 1535–1542.
7 A. S. Yasin, A. Y. Mohamed, I. M. A. Mohamed, D. Y. Cho, C. H. Park and C. S. Kim, *Chem. Eng. J.*, 2019, **371**, 166–181.
8 J. Oladunni, J. H. Zain, A. Hai, F. Banat, G. Bharath and E. Alhseinat, *Sep. Purif. Technol.*, 2018, **207**, 291–320.
9 D. D. Caudle, *Sci. Rep.*, 1966, **4**, 7397.
10 A. Johnson, A. Venolia, J. Newman, R. Wilbourne, C. Wong and W. Gillam, *Electrosorb process for desalting water*, 1970, vol. 200, p. 056.
11 M. S. Gaikwad, C. Balomajumder and A. K. Tiwari, *Chemosphere*, 2020, **254**, 126781.
12 J. Sun, L. Liu and F. Yang, *J. Hazard. Mater.*, 2020, **394**, 122534.
13 D. Li, X. Ning, Y. Yuan, Y. Hong and J. Zhang, *J. Environ. Sci.*, 2020, **91**, 62–72.
14 S. M. Jung, J. H. Choi and J. H. Kim, *Sep. Purif. Technol.*, 2012, **98**, 31–35.
15 X. Xu, Y. Liu, M. Wang, C. Zhu, T. Lu, R. Zhao and L. Pan, *Electrochim. Acta*, 2016, **193**, 88–95.
16 C. Yan, Y. W. Kanaththage, R. Short, C. T. Gibson and L. Zou, *Desalination*, 2014, **344**, 274–279.
17 R. Zhao, P. M. Biesheuvel and H. Miedema, *J. Phys. Chem. Lett.*, 2010, **1**, 205–210.
18 R. Zhao, P. Biesheuvel and A. Van der Wal, *Energy Environ. Sci.*, 2012, **5**, 9520–9527.
19 J. Cao, Y. Wang, C. Chen, F. Yu and J. Ma, *J. Colloid Interface Sci.*, 2018, **518**, 69–75.
20 P. Liu, H. Wang, T. Yan, J. Zhang, L. Shi and D. Zhang, *J. Mater. Chem. A*, 2016, **4**, 5303–5313.
21 H. Wang, T. Yan, P. Liu, G. Chen, L. Shi, J. Zhang, Q. Zhong and D. Zhang, *J. Mater. Chem. A*, 2016, **4**, 4908–4919.
22 H. Duan, T. Yan, Z. An, J. Zhang, L. Shi and D. Zhang, *RSC Adv.*, 2017, **7**, 39372–39382.
23 M. A. Radi, E. T. Sayed, H. Alawadhi and M. A. Abdelkareem, *Crit. Rev. Environ. Sci. Technol.*, 2021, **52**, 3080–3136.
24 L. Chang, Y. Fei and Y. Hu, *J. Mater. Chem. A*, 2021, **9**, 1429.
25 J. M. A. Freire, J. J. Lado, E. García-Quismondo, G. C. Burillo, J. Palma, A. R. Loiola, E. Longhinotti and M. A. Anderson, *Sep. Purif. Technol.*, 2021, **273**, 118977.
26 K. M. Barcelos, K. S. G. C. Oliveira and L. A. M. Ruotolo, *Desalination*, 2020, **492**, 114594.
27 R. L. Ornitta, F. J. García-Mateos, J. J. Lado, J. Rodríguez-Mirasol, T. Cordero, P. Hammer and L. A. Ruotolo, *Carbon*, 2017, **123**, 318–333.
28 W. Cai, J. Yan, T. Hussin and J. Liu, *Electrochim. Acta*, 2017, **225**, 407–415.
29 J. Duan, S. Bao and Y. Zhang, *Chem. Eng. Res. Des.*, 2018, **132**, 178–186.
30 X. Xu, H. Tang, M. Wang, Y. Liu, Y. Li, T. Lu and L. Pan, *J. Mater. Chem. A*, 2016, **4**, 16094–16100.
31 Y. Liu, X. Xu, M. Wang, T. Lu, Z. Sun and L. Pan, *Chem. Commun.*, 2015, **51**, 12020–12023.
32 S. Zhao, T. Yan, H. Wang, G. Chen, L. Huang, J. Zhang, L. Shi and D. Zhang, *Appl. Surf. Sci.*, 2016, **369**, 460–469.
33 Y. Li, J. Qi, J. Li, J. Shen, Y. Liu, X. Sun, J. Shen, W. Han and L. Wang, *ACS Sustainable Chem. Eng.*, 2017, **5**, 6635–6644.
34 R. Kumar, S. S. Gupta, S. Katiyar, V. K. Raman, S. K. Varigala, T. Pradeep and A. Sharma, *Carbon*, 2016, **99**, 375–383.
35 I. Yang, S. G. Kim, S. H. Kwon, M. S. Kim and J. C. Jung, *Electrochim. Acta*, 2017, **223**, 21–30.
36 Y. Yang, Y. Hao, X. Wang, Q. Yan, J. Yuan, Y. Shao, L. Niu and S. Huang, *Electrochim. Acta*, 2015, **167**, 364–371.
37 J. Liao, Q. Hu, Y. Yu, H. Wang, Z. Tang, Z. Wen and C. Chen, *J. Mater. Chem. A*, 2017, **5**, 19017–19024.
38 W. Shi, H. Li, X. Cao, Z. Y. Leong, J. Zhang, T. Chen, H. Zhang and H. Y. Yang, *Sci. Rep.*, 2016, **6**, 18966.
39 C. Macías, G. Rasines, P. Lavela, M. C. Zafra, J. L. Tirado and C. O. Ania, *ACS Sustainable Chem. Eng.*, 2016, **4**, 2487–2494.
40 Y. Liao, M. Wang and D. J. Chen, *J. Radioanal. Nucl. Chem.*, 2018, **316**, 635–647.
41 X. Xu, Z. Sun, D. H. Chua and L. Pan, *Sci. Rep.*, 2015, **5**, 11225.
42 M. Wang, X. Xu, J. Tang, S. Hou, M. S. A. Hossain, L. Pan and Y. Yamauchi, *Chem. Commun.*, 2017, **53**, 10784–10787.
43 S. W. Bokhari, A. H. Siddique, P. C. Sherrell, X. Yue, K. M. Karumbaiah, S. Wei, A. V. Ellis and W. Gao, *Energy Rep.*, 2020, **6**, 2768–2784.
44 Z. Y. Leong, G. Lu and H. Y. Yang, *Desalination*, 2019, **451**, 172–181.
45 W. Chang, P. Chen, W. Chen, S. Liu and H. P. Wang, *Environ. Chem.*, 2021, **18**, 352–359.
46 H. Li, L. Zou, L. Pan and Z. Sun, *Environ. Sci. Technol.*, 2010, **44**, 8692–8697.
47 D. J. Ahirrao and N. Jha, *Carbon*, 2019, **152**, 837–850.
48 J. Ma, L. Wang and F. Yu, *Electrochim. Acta*, 2018, **263**, 40–46.
49 X. Xu, Y. Liu, T. Lu, Z. Sun, D. H. C. Chua and L. K. Pan, *J. Mater. Chem. A*, 2015, **3**, 13418–13425.
50 Y. Liu, C. Nie, X. Liu, X. Xu, Z. Sun and L. Pan, *RSC Adv.*, 2015, **5**, 15205–15225.
51 H. Duan, T. Yan, G. Chen, J. Zhang, L. Shi and D. Zhang, *Chem. Commun.*, 2017, **53**, 7465–7468.

52 H. Wang, D. Zhang, T. Yan, X. Wen, J. Zhang, L. Shi and Q. Zhong, *J. Mater. Chem. A*, 2013, **1**, 11778–11789.
53 A. Amiri, G. Ahmadi, M. Shanbedi, M. Savari, S. N. Kazi and B. T. Chew, *Sci. Rep.*, 2015, **5**, 17503.
54 X. Wu, K. Li, S. Ying, L. Liu, M. Wang and Y. Liao, *J. Radioanal. Nucl. Chem.*, 2019, **321**, 977–984.
55 J. Li, B. Ji, R. Jiang, P. Zhang, N. Chen, G. Zhang and L. Qu, *Carbon*, 2018, **129**, 95–103.
56 M. S. Zoromba, M. H. Abdel-Aziz, M. Bassyouni, S. Gutub, D. Demko and A. Abdelkader, *ACS Sustainable Chem. Eng.*, 2017, **5**, 4573–4581.
57 J. Feng, L. Liu and Q. Meng, *J. Colloid Interface Sci.*, 2021, **582**, 447–458.
58 X. Liu, L. Liu, J. Zhang and Q. Meng, *Colloids Surf., A*, 2021, **618**, 126463.
59 Y. Belaustegui, I. Rincón, F. Fernández-Carretero, P. Azpiroz, A. García-Luís and D. A. P. Tanaka, *Chem. Eng. J. Adv.*, 2021, **6**, 100094.
60 L. Chang and Y. H. Hu, *J. Phys. Chem. Solids*, 2019, **134**, 64–68.
61 Z. U. Khan, T. Yan, L. Shi and D. Zhang, *Environ. Sci.: Nano*, 2018, **5**, 980–991.
62 P. Liu, T. Yan, J. Zhang, L. Shi and D. Zhang, *J. Mater. Chem. A*, 2017, **5**, 14748–14757.
63 G. Bharath, E. Alhseinat, N. Ponpandian, M. A. Khan, M. R. Siddiqui, F. Ahmed and E. H. Alsharaeh, *Sep. Purif. Technol.*, 2017, **188**, 206–218.
64 O. Noonan, Y. Liu, X. Huang and C. Yu, *J. Mater. Chem. A*, 2018, **6**, 14272–14280.
65 Y. Zhang, L. Chen, S. Mao, Z. Sun, Y. Song and R. Zhao, *J. Colloid Interface Sci.*, 2019, **5**, 252–260.
66 X. Wen, D. Zhang, T. Yan, J. Zhang and L. Shi, *J. Mater. Chem. A*, 2013, **1**, 12334–12344.
67 Y. Zhu, G. Zhang, C. Xu and L. Wang, *ACS Appl. Mater. Interfaces*, 2020, **12**, 29706–29716.
68 V. S. Wadi, Y. Ibrahim, A. F. Arangadi, A. Kilybay, M. O. Mavukkandy, E. Alseinat and S. Hasan, *J. Electroanal. Chem.*, 2022, **914**, 116318.
69 J. P. L. Lazarte, L. Bautista-Patacsil, R. C. P. Eusebio, A. H. Orbecido and R. A. Doong, *Nanomaterials*, 2019, **9**, 1319.
70 S. Han, Z. Li, S. Ma, Y. Zhi, H. Xia, X. Chen and X. Liu, *J. Mater. Chem. A*, 2021, **9**, 3333–3340.
71 M. Mao, T. Yan, G. Chen, J. Zhang and D. Zhang, *Environ. Sci. Technol.*, 2021, **55**, 730–737.
72 J. Han, T. Yan, J. Shen, L. Shi, J. Zhang and D. Zhang, *Environ. Sci. Technol.*, 2019, **53**, 12668–12676.
73 Y. H. Liu, H. C. Hsi, K. C. Li and C. H. Hou, *ACS Sustainable Chem. Eng.*, 2016, **4**, 4762–4770.
74 J. P. L. Lazarte, R. C. Dipasupil, G. Y. S. Pasco, R. C. P. Eusebio, A. H. Orbecido, R. A. Doong and L. Bautista-Patacsil, *Nanomaterials*, 2018, **8**, 934.
75 G. Divyapriya, K. K. Vijayakumar and I. Nambi, *Desalination*, 2019, **451**, 102–110.
76 M. A. Jaoude, E. Alhseinat, K. Polychronopoulou, G. Bharath, I. F. F. Darawsheh, S. Anwer, M. A. Baker, S. J. Hinder and F. Banat, *Electrochim. Acta*, 2020, **330**, 135202.
77 G. Bharath, N. Arora, A. Hai, F. Banat, D. Savariraj, H. Taher and R. V. Mangalaraja, *Electrochim. Acta*, 2020, **337**, 135668.
78 K. Xie, J. Yu, X. Zhang, S. Hu, R. Liu, H. Song, J. Shen, Y. Wang, A. Li and S. Zhang, *Chem. Eng. J.*, 2021, **414**, 128747.
79 T. Li and H. Liu, *Powder Technol.*, 2018, **327**, 275–281.
80 Z. Ji, X. Shen, H. Zhou and K. Chen, *Ceram. Int.*, 2015, **41**, 8710–8716.
81 A. Yousef, A. M. Al-Enizi, I. M. A. Mohamed, M. M. El-Halwany, M. Ubaidullah and R. M. Brooks, *Ceram. Int.*, 2020, **46**, 15034–15043.
82 R. Wang, B. Xu, Y. Chen, X. Yin, Y. Liu and W. Yang, *Sep. Purif. Technol.*, 2022, **282**, 120122.
83 G. Luo, L. Gao, D. Zhang, J. Zhang and T. Lin, *Desalin. Water Treat.*, 2018, **135**, 157–166.
84 L. Chong, P. Chen, J. Huang, H. Huang and H. P. Wang, *Chemosphere*, 2018, **191**, 296–301.
85 C. Zhang, X. Wang, H. Wang, X. Wu and J. Shen, *Processes*, 2019, **7**, 29.
86 K. Mohanapriya and N. Jha, *Electrochim. Acta*, 2019, **324**, 134870.
87 J. Cao, Y. Wang, C. Chen, F. Yu and J. Ma, *J. Colloid Interface Sci.*, 2018, **518**, 69–75.
88 A. S. Yasin, A. Y. Mohamed, D. H. Kim, T. L. L. Doan, S. S. Chougule, N. Jung, S. Nam and K. Lee, *Sep. Purif. Technol.*, 2021, **277**, 119428.
89 W. Dianbudiyanto and S. H. Liu, *Desalination*, 2019, **468**, 114069.
90 D. Zhang, T. Yan, L. Shi, X. Wen and J. Zhang, *J. Mater. Chem.*, 2012, **22**, 14696–14704.
91 D. Zhang, X. Wen, L. Shi, T. Yan and J. Zhang, *Nanoscale*, 2012, **4**, 5440–5446.
92 T. Yan, J. Liu, H. Lei, L. Shi, Z. An, H. S. Park and D. Zhang, *Environ. Sci.: Nano*, 2018, **5**, 2722.
93 H. Wang, C. Zhang, Z. Liu, L. Wang, P. Han, H. Xu, K. Zhang, S. Dong, J. Yao and G. Cui, *J. Mater. Chem.*, 2011, **21**, 5430–5434.
94 S. Liu, B. Li, Y. Zhou, X. Xu, R. Yang, Q. Wang and J. Li, *J. Mater. Res. Technol.*, 2021, **15**, 1996–2006.
95 G. Zhang, W. Li, Z. Chen, J. Long and C. Xu, *Carbon*, 2022, **18**, 86–96.
96 Z. U. Khan, T. Yan, J. Han, L. Shi and D. Zhang, *Environ. Sci.: Nano*, 2019, **6**, 3442–3453.
97 X. Gu, Y. Deng and C. Wang, *ACS Sustainable Chem. Eng.*, 2016, **5**, 325–333.
98 M. Mi, X. Liu, W. Kong, Y. Ge, W. Dang and J. Hu, *Desalination*, 2019, **464**, 18–24.
99 Y. Li, J. Qi, J. Li, J. Shen, Y. Liu, X. Sun, J. Shen, W. Han and L. Wang, *ACS Sustainable Chem. Eng.*, 2017, **5**, 6635–6644.
100 Y. Liu, X. Xu, M. Wang, T. Lu, Z. Sun and L. Pan, *J. Mater. Chem. A*, 2015, **3**, 17304–17311.
101 H. Lei, T. Yan, H. Wang, L. Shi, J. Zhang and D. Zhang, *J. Mater. Chem. A*, 2015, **3**, 5934–5941.
102 H. Wang, D. Zhang, T. Yan, X. Wen, L. Shi and J. Zhang, *J. Mater. Chem.*, 2012, **22**, 23745–23748.

103 H. Wang, L. Shi, T. Yan, J. Zhang, Q. Zhong and D. Zhang, *J. Mater. Chem. A*, 2014, **2**, 4739–4750.
104 J. Kim, W. H. Khoh, B. H. Wee and J. D. Hong, *RSC Adv.*, 2015, **5**, 9904–9911.
105 G. Lui, G. Li, X. Wang, G. Jiang, E. Lin, M. Fowler, A. Yu and Z. Chen, *Nano Energy*, 2016, **24**, 72–77.
106 Y. Wu, G. Jiang, G. Liu, G. Lui, Z. Cano, Q. Li, Z. Zhang, A. Yu, Z. Zhang and Z. Chen, *J. Mater. Chem. A*, 2019, **7**, 15633–15639.
107 Y. Wu, G. Jiang, Q. Li, Z. Zhang and Z. Chen, *RSC Adv.*, 2019, **9**, 28186–28193.
108 K. A. Khalil, N. A. M. Barakat, M. Motlak and F. S. Al-Mubadde, *Sci. Rep.*, 2020, **10**, 9676.
109 X. Liu, Y. Liu, Y. Wang, D. Yuan, C. Wang and J. Liu, *J. Solid State Electrochem.*, 2021, **25**, 2443–2454.
110 X. Liu, Y. Liu, Y. Wang, D. Yuan, J. Liu and Z. Zhu, *J. Electrochem. Soc.*, 2021, **168**, 066514.
111 D. Han, C. Zhang, J. Guan, L. Gai, R. Yue, L. Liu, M. Afzal, C. Song, S. Wang and X. Sun, *Electrochim. Acta*, 2020, **336**, 135639.
112 G. S. S. Mamaril, M. D. G. de Luna, K. Bindumadhavan, D. C. Ong, J. A. I. Pimentel and R. A. Doong, *Sep. Purif. Technol.*, 2021, **272**, 117559.
113 Y. Liu, X. Tang, L. Zhou, Z. Liu, J. Ouyang, L. Dai, Z. Le and A. A. Adesina, *Sep. Purif. Technol.*, 2022, **290**, 120827.
114 Y. Liao, C. Yan, K. Zeng, C. Liao and M. Wang, *Chem. Eng. J.*, 2021, **424**, 130351.
115 L. Chen and D. G. Tong, *Sep. Purif. Technol.*, 2020, **250**, 117175.
116 X. Tang, L. Zhou, H. Yu, Y. Dai, J. Ouyang, Z. Liu, Y. Wang, Z. Le and A. A. Adesina, *Sep. Purif. Technol.*, 2022, **278**, 119604.
117 J. Ma, L. Wang, F. Yu and X. Dai, *Chem. Eng. J.*, 2019, **370**, 938–943.
118 F. Zhou, T. Gao, M. Luo and H. Li, *Chem. Eng. J.*, 2018, **343**, 8–15.
119 L. Chen, C. Wang, S. Liu, Q. Hu, L. Zhu and C. Cao, *Chemosphere*, 2018, **193**, 989–997.
120 C. Zhang, J. Guan, L. Liu, Z. Wan, S. Wang and X. Sun, *Desalination*, 2021, **500**, 114846.
121 T. Wang, H. Liang, L. Bai, B. Liu, X. Zhu, J. Wang, J. Xing, N. Ren and G. Li, *J. Electrochem. Soc.*, 2020, **167**, 043501.
122 G. Wang, T. Yan, J. Shen, J. Zhang and D. Zhang, *Environ. Sci. Technol.*, 2021, **55**, 11979–11986.
123 G. Wang, T. Yan, J. Shen, J. Zhang, L. Shi and D. Zhang, *Environ. Sci.: Nano*, 2021, **8**, 122–130.
124 M. Mao, T. Yan, J. Shen, J. Zhang and D. Zhang, *Environ. Sci. Technol.*, 2021, **55**, 7665–7673.
125 L. Huang, T. Yan, A. E. D. Mahmoud, S. Li, j. Zhang, L. Shi and D. Zhang, *Environ. Sci.: Nano*, 2021, **8**, 950–959.
126 H. Wang, T. Yan, J. Shen, J. Zhang, L. Shi and D. Zhang, *Environ. Sci.: Nano*, 2020, **7**, 317–326.
127 G. Wang, T. Yan, J. Zhang, L. Shi and D. Zhang, *Environ. Sci. Technol.*, 2020, **54**, 8411–8419.
128 Z. Bo, Z. Huang, C. Xu, Y. Chen, E. Wu, J. Yan, K. Cen, H. Yang and K. Ostrikov, *Energy Storage Mater.*, 2022, **50**, 395–406.
129 M. Zhang and W. Kong, *J. Electroanal. Chem.*, 2020, **878**, 114703.
130 O. Sufiani, J. Elisadiki, R. L. Machunda and Y. A. C. Jande, *J. Electroanal. Chem.*, 2019, **848**, 113328.